Title

Full title: Strong immobilization of *C. elegans* en masse on cultivation plates by thermoelectric cooling for high-throughput submicron-resolution microscopy

Short title: Cooling immobilization for microscopy

Headline

Straightforward immobilization of entire *C. elegans* populations enables high-throughput microscopy at submicron resolution.

Authors

Yao L. Wang[1†], Erik L. Jaklitsch[1†], Noa W. F. Grooms[1], Leilani G. Schulting[1], Samuel H. Chung[1]*

[†]Co-first author

*Corresponding author, E-mail: schung@northeastern.edu

Affiliations

[1]Department of Bioengineering, Northeastern University, Boston, Massachusetts, USA

Abstract

High-resolution *in vivo* microscopy has profoundly impacted our understanding of development and disease by revealing anatomy and molecular targets at the subcellular level. Unfortunately, many microscopy approaches remain low-throughput because current immobilization techniques for precise imaging require significant manual effort. To greatly

improve the throughput of subcellular resolution imaging in the nematode *Caenorhabditis elegans*, we implement a novel cooling method to easily immobilize entire populations directly on their native cultivation plates. Previous studies immobilized animals in liquid media between 1-4 °C, which allows animal motion and blurs images. Counterintuitively, we find that cooling to 5-7 °C immobilizes animals much more effectively, enabling clear submicron-resolution fluorescence imaging. We demonstrate 64× magnification 3D image stacks and 2-min long timelapse recordings of the ASJ neuron without image blur. We estimate that the time spent on animal preparation and recovery under our cooling approach is 98% less than under a typical azide immobilization approach. Our simple, yet robust cooling platform enables high-throughput and high-resolution microscopy with minimal user effort. By obviating the need for individual animal manipulation, this approach could also empower automated imaging of large *C. elegans* populations within standard experimental setups and workflows.

Introduction

The nematode *C. elegans* is a widely-utilized model organism for studying many biological processes. Similar to microorganisms, *C. elegans* are typically cultivated on agarose plates, and they reproduce rapidly by self-fertilization, making them well-suited for studies that require a large sample size. Their transparency and a wide array of labelling techniques allows straightforward visualization of their internal anatomy. Many studies in *C. elegans* image subcellular structures at submicron resolution, which necessitates animal immobilization to prevent image blur. Proper immobilization is especially crucial for techniques involving multiple images in space or time, such as 3D image stacks (*i.e.*, z-

stacks) and timelapse imaging. Typically, immobilization involves manual manipulation of individual animals and mounting them on slides. These time- and labor-intensive procedures restrict experiments to small sample sizes.

Though many strategies have been developed to immobilize *C. elegans*, there are distinct drawbacks for each (see Table S1). In brief, chemical methods utilize agents such as sodium azide or levamisole to immobilize by disrupting animal physiology (Reeve, 1988). Mechanical methods, such as polystyrene beads and hydrogel mixtures, physically restrain animals by pressure, viscosity, or friction (Kim, *et al.*, 2013). Microfluidic and on-chip technologies constrain animals by pressure, compression, or suction against a membrane/wall or fluid (Guo, *et al.*, 2008; Zeng, *et al.*, 2008). Lastly, extreme temperatures can also immobilize animals, and most techniques cool animals in flooded wells or microfluidics (Rohde and Yanik, 2011). Despite the many advances in novel immobilization strategies, several significant drawbacks remain: Some of the above strategies require fabrication of slides and significant manual pre- and post-processing of individual animals. They may increase physiological or physical stress on animals (Manjarrez and Mailler, 2020). Some strategies require complex fabrication and setups or require significant user training. Several methods may also allow small animal movements that blur images, particularly in the nose and pharynx. Notably, none of the current strategies allow for direct imaging on cultivation plates, necessitating time-consuming animal transfer.

class	examples	mechanism of action	drawbacks
chemical	sodium azide	block adenosine triphosphate production (Reeve, 1988; Bowler, *et al.*, 2006; Manjarrez and Mailler, 2020)	labor-intensive pre- and post-processing, stress-related secondary effects (Massie, *et al.*, 2003; Manjarrez and Mailler, 2020)
	levamisole	acetylcholine receptor overstimulation at neuromuscular junction (Brenner, 1974; Robertson, *et al.*, 2010; Puttachary, *et al.*, 2010; Martin, *et al.*, 2012)	labor-intensive pre- and post-processing, may impact viability and morphology, stress-related secondary effects, levamisole-resistant mutations (Martin, *et al.*, 2012)
mechanical	nanoparticle / microbead	pressure, friction (Kim, *et al.*, 2013)	requires slide mounting, small movements persist, can cause permanent damage, animals not accessible during immobilization (Kim, *et al.*, 2013)
	Pluronic F127 hydrogel (often used with microbead matrices)	viscosity, friction (Shachaf, *et al.*, 2010; Basak and Bandyopadhyay, 2013; Krajniak and Lu, 2010)	labor-intensive pre- and post-processing, forward-backward locomotion and other small movements persist (Krajniak and Lu, 2010; Krajniak, *et al.*, 2013; Dong, *et al.*, 2018)
	microfluidics, on-chip technologies	controlled flow, compression, suction (Chronis, *et al.*, 2007; Lockery, 2007; Zeng, *et al.*, 2008; Hulme, *et al.*, 2007; Guo, *et al.*, 2008; Ben-Yakar, *et al.*, 2009; Chronis, 2010; Crane, *et al.*, 2010)	complex setup, setup designed for specific applications, small movements persist (Chronis, *et al.*, 2007; Lockery, 2007; Ben-Yakar, *et al.*, 2009; Chronis, 2010)
extreme temperature	2-4 °C cooling in multiwell or microfluidic	undefined cooling effects (Chung, *et al.*, 2008; Rohde and Yanik, 2011)	stress-related secondary effects, may cause damage to animal cells, small movements persist (Chung, *et al.*, 2008)
	37 °C heating	light-induced heat knockdown (Chuang, *et al.*, 2013)	complex setup, stress-related secondary effects, high fatality under multiple immobilizations (Chuang, *et al.*, 2013)

Table S1. Existing immobilization methods grouped by class and mechanism. Note that those techniques are often combined.

Here we address these shortcomings by developing an approach that readily and reversibly immobilizes entire animal populations with minimal user effort. We detail the successful operation of a thermoelectric cooling stage and associated methods that can immobilize *C. elegans* en masse directly on cultivation plates for high-resolution imaging. We describe

our cooling instrument, which stably holds the entire cultivation plate at a desired temperature. We characterize animal movement at several target temperatures and under different cooling rates. Surprisingly, we found that cooling to relatively higher temperatures, specifically 6 °C, minimizes animal movement, though previously-reported cooling strategies utilized temperatures between 2-4 °C (Rohde and Yanik, 2011; Chung, *et al.*, 2008). Animal movement while cooled consists of bouts of submicron nose tip movement occurring infrequently enough to permit high-resolution brightfield imaging during timescales on the order of minutes. Cooling for short-term immobilization does not impact *C. elegans* fecundity or lifespan. Finally, using our novel immobilization method, we obtain submicron-resolution z-stacks and timelapse fluorescence images of *C. elegans* neurons without blurring from animal motion. Our approach greatly accelerates the pace of high-resolution imaging in *C. elegans*, and we envision that it could form the basis for automated imaging of large *C. elegans* populations on common experimental setups and workflows.

Results

Cooling stage apparatus and temperature distribution

Our design goal is to uniformly cool an entire 55-mm diameter agar cultivation plate to a target temperature, immobilizing animals for high-resolution fluorescence imaging while also preserving transillumination and access to animals. Agar plates are commonly used for cultivating, observing, and manipulating *C. elegans*, so our instrument has broad applicability. As shown in Fig. 1ab, our instrument comprises a thin stage made of an 80-mm diameter sapphire window, a thermally-conductive copper body, a thermoelectric Peltier heat pump, and a closed-loop liquid cooler. The sapphire window is transparent for

transillumination and has a high thermal conductivity. We designed notch cut-outs on the colder side of the sapphire window to improve temperature uniformity across the window. The Peltier is a thermoelectric, solid-state device that pumps heat between its two sides depending on applied voltage.

The stage rapidly cools agar plates resting on the sapphire window. Heat leaves the plate to the sapphire window and then transfers to the copper body and Peltier. The Peltier pumps heat to the closed-loop cooler for removal. Thermal simulation of our design predicted a uniform thermal distribution (< 1°C temperature difference from target temperature, T_{set}) across the central 40 mm-diameter area of the cultivation plate (Fig. 1b thermal simulation top view). We constructed, assembled, and preliminarily tested the device (Fig. 1c) by achieving and holding a variety of temperatures on the agar surface. We measured the thermal distribution of the agar plate and cooling stage, demonstrating an even distribution across the plate's central area and ensuring that the animals are held at the same temperature for uniform immobilization (Fig. 1d). Thus, our device features include optical transparency for transillumination, high thermal conductivity for cooling efficiency, and uniform temperature distribution across the agar surface.

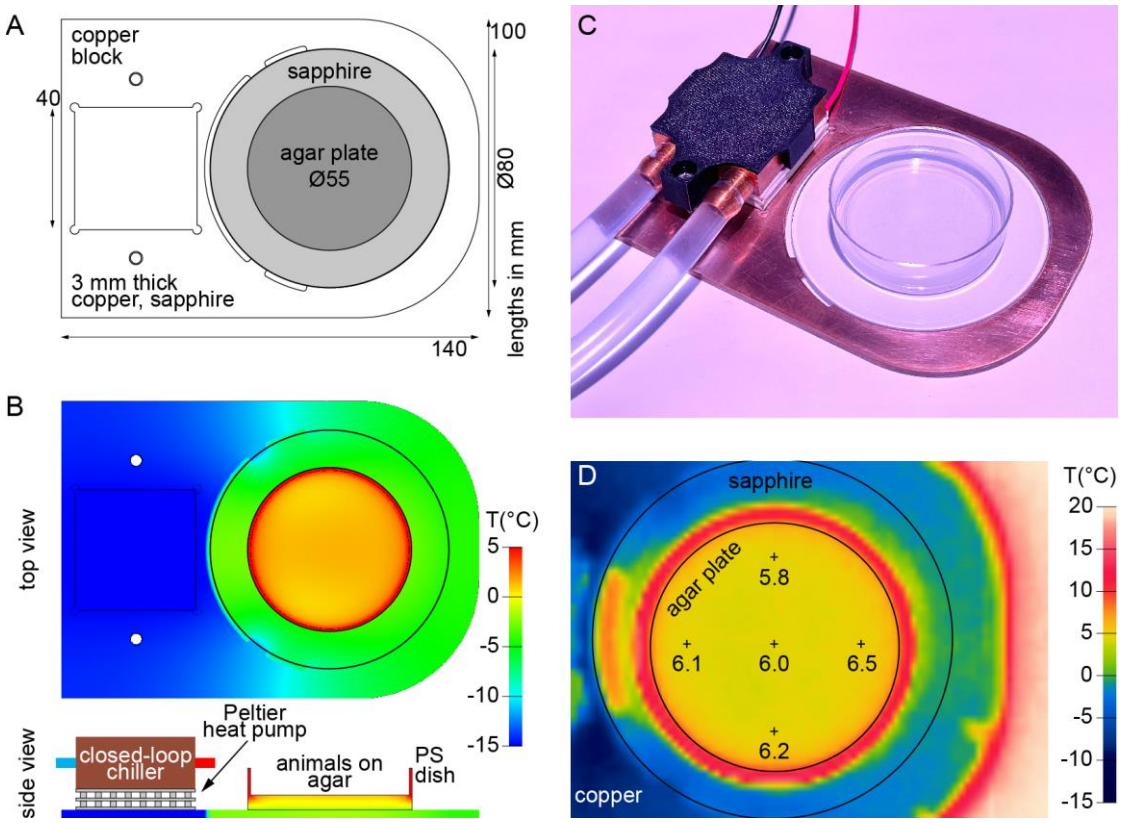

Fig. 1. Cooling stage apparatus. (a) Top-down view of cooling immobilization stage. Agar cultivation plates placed on the sapphire window. (b) Thermal modeling of stage and agar plate. Peltier heat pump and liquid cooling system secured to the copper base. (c) Photograph of cooling stage and agar plate. (d) Thermal image of unlidded agar plate and stage cooled to T_{set} = 6 °C obtained by infrared camera. Temperatures at indicated points.

General observations of cooling immobilization on agarose plates

Because our study is the first, to our knowledge, to immobilize animals on agar plates by cooling, we began by carefully characterizing the impact of temperature on animal movement. At temperatures ≥ 8 °C, most animals are not immobilized and crawl out of the imaging field of view within minutes. Similar to prior studies of animals in liquid solution, cooling to 1-7 °C slows *C. elegans* movement and stops crawling on plates immediately. By eye, the part of the animal that moves the most under cooling immobilization is the nose. Pharyngeal pumping is strongly suppressed, the tail also shows some movement, and the body moves the least. Movie S1 shows typical examples of immobilized animal

movement at 6 °C, where we immobilized three N2 wild-type worms on a cultivation plate. The video rate is sped up 50× to show a 1200-s timespan in a 24-s video. The body parts are immobilized to varying levels, consistent with the independent control of these parts (Alkema, *et al.*, 2005) and our experience with sodium azide anesthesia (Chung, *et al.*, 2013a). Because the nose tip exhibits the most movement and contains our target neuron, we verify our cooling immobilization by measuring movement of the nose tip throughout our work described below.

Optimal cooling temperature for immobilization

We next determined the optimal target temperature, T_{set}, to immobilize animals. Previous reports utilized target temperatures of 2-4 °C (Rohde and Yanik, 2011; Chung, *et al.*, 2008) but presented minimal quantitative or qualitative characterization of movement. In our experience, some animal movement, however slow or small, persists at all temperatures. We have even observed movement of animals in supercooled buffer held well below 0 °C. By cooling plates to 1-7 °C using our instrument, we investigated animal immobilization in response to a wide temperature range. Surprisingly, we found that a relatively higher temperature, 6 °C, is the optimal temperature for immobilization. Figure 2 shows average nose tip velocity for each minute at specified times after reaching T_{set}. At 1-3 °C, nose movement velocity is slow initially but does not greatly decrease over the hour after reaching T_{set} (Fig. 2a). We confirmed that this persistent velocity trend continued for at least 2 h after reaching T_{set} (see below for details). At these velocities (0.5-1.0 μm/s), we could not obtain clear high-resolution images, even with our advanced microscope and sensitive camera. 4 °C represents a transition temperature, where velocity is high initially but decreases to speeds comparable to those at 1-3 °C. At 5-7 °C, velocity is high initially

but, decreases to very low levels after ~50 min at T_{set}. This immobilization appears to take effect progressively over time, in contrast to the immediate immobilization at lower temperatures and earlier times. The velocities at 50-60 min are significantly ($p << 0.001$) below those at 1-3 °C and near or below our resolution limit. As a result, this minimal velocity (< 0.5 μm/s) permits clear submicron-resolution microscopy (see below). Because the final velocities are similar between 5-7 °C, we selected 6 °C as the T_{set} for further study.

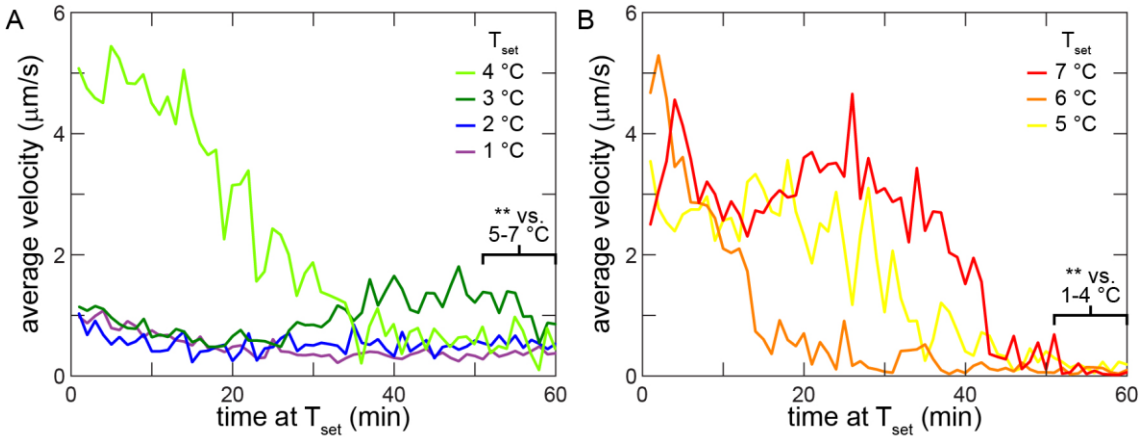

Fig. 2. Relatively higher temperatures immobilize animals more effectively. Average nose tip velocity each minute for (a) low temperature (1-4 °C) and (b) high temperature (5-7 °C) under fast cooling immobilization. $n = 6$ animals. $p < 0.001$ (**) comparing final 10 min of movement for 1-4 °C and 5-7 °C.

Different cooling rates produce similar immobilization

We next examined the impact of the cooling rate on immobilization by testing three methods to cool animals down to 6 °C at different rates. We term these methods "slow", "fast", and "abrupt". Figure 3 shows plate cooling profiles for slow and fast cooling methods. Slow cooling uses a typical 4 °C refrigerator to cool down a lidded cultivation plate to 6 °C in about 50-60 mins. After this first hour in the refrigerator, we transfer this plate to the cooling stage that is pre-cooled, to maintain animals at 6 °C. In fast cooling, we place a plate directly onto the cooling stage to bring the plate from 20 °C to 6 °C. The

cooling stage can maintain colder temperatures than the refrigerator; thus, it can cool down animals to 6 °C within 15 mins. Abrupt cooling requires more user effort: we pick animals from their original 20 °C plate directly to a pre-cooled 6 °C plate. Based on strong thermal conductivity and small animal size, we expect animals are cooled to 6 °C in seconds.

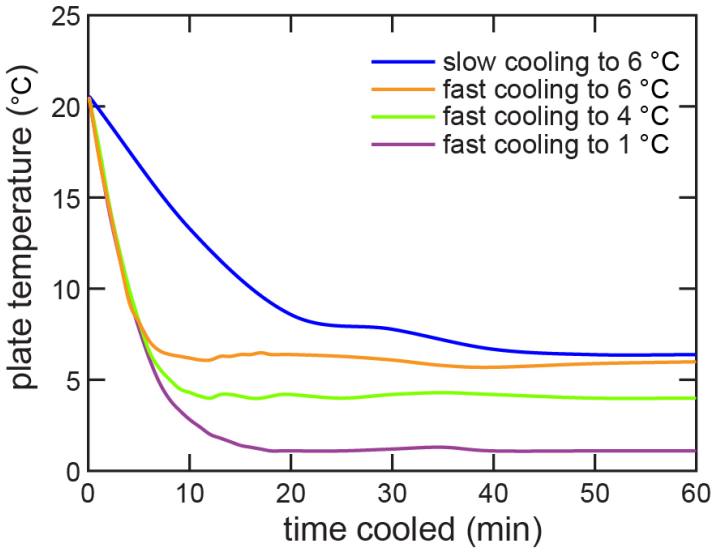

Fig. 3. Plate cooling profiles. Plate temperatures over time for different cooling methods and T_{set}.

As previously stated, immobilization at higher T_{set} is strongest starting ~50 min after beginning of cooling, and the first hour of slow cooling is in the refrigerator. Thus, we measured velocity for an extended length of time, beginning when the animals reached T_{set} and up to 2 h from the start of cooling (Fig. 4). We compared abrupt, fast, and slow cooling to 6 °C and fast cooling to 1 °C. After cooling to 6 °C, we observe no significant differences in velocity during the 80-120 min range between slow and fast cooling (p = 0.08) or between slow and abrupt cooling (p = 0.32), indicating that the cooling rate does not require careful tuning to optimize immobilization. By contrast, in agreement with our prior results (Fig. 2), fast cooling to 1 °C allows significantly more movement during the 80-120 min range than fast cooling to 6 °C (p < 0.001). Of the three cooling methods, slow cooling

involves the least amount of user time and effort (details in Materials and methods). While certain experiments may require fast or abrupt cooling, we favor the slow cooling method and utilize it for the remainder of this study.

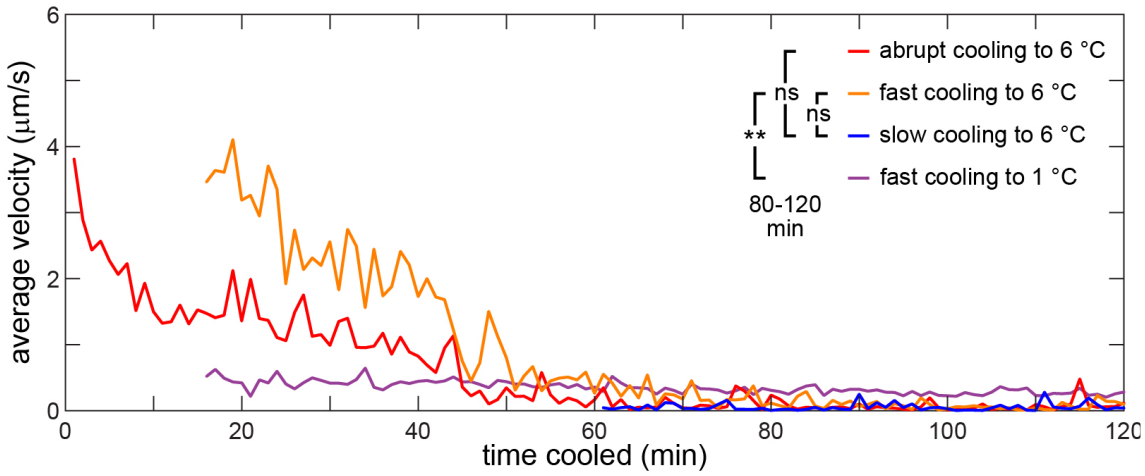

Fig. 4. Different cooling rates to 6 °C eventually immobilize similarly. Average velocity of nose tip movement for abrupt, fast, and slow cooling methods to 6 °C and fast cooling to 1 °C. Note that fast and slow cooling velocity measurement begins after cooling initiation to allow animals to reach T_{set}. n = 6 animals for each condition. $p < 0.001$ (**) and not significant (ns) comparisons of movement during 80-120 min.

Intermittent nose movements under cooling.

The goal of our device development is to immobilize animals for imaging, especially for high-resolution microscopy. As such, we ascertained if animals were sufficiently immobilized for imaging by our cooling stage. We measured nose movements each second to better quantify immobilization behavior. Figure 5a shows second-by-second measurements of typical nose movement under 6 °C slow cooling. Similar to sleep and lethargus (Raizen, *et al.*, 2008; Iwanir, *et al.*, 2013), nose movement under cooling conditions is intermittent, mostly comprised of seconds-long "bouts" of increased activity separated by "windows" with little to no movement. We characterized the distance moved during bouts and the length of the windows. Only 1.4% of movements surpass 1 μm, and

95% of measurements yielded movement below the resolution limit (0.5 μm) (Fig. 5b). Movements below 1 μm do not produce visible blur even at the highest magnification of our microscope (64×) because the motion is largely confined to the tip. Also, most of the experiment duration is contained within longer windows: 96% of the duration is part of windows that are longer than 0.5 min, and 90% of the time is part of windows that are longer than 1 min (Fig. 5c). This level of movement is sufficiently low to image by eye and is also amenable to high-resolution, blur-free brightfield imaging by a camera, which can be performed at most timepoints. Moreover, technology improvements have produced increasingly brighter fluorescent labels, enhanced optics, and efficient cameras. If these tools allow rapid and more sensitive image acquisition, the immobilization requirements may be relaxed. For instance, partial immobilization, achievable at earlier times, may be sufficient for imaging with improved technologies, allowing high-speed repetitive immobilizations for longitudinal imaging. In summary, our cooling immobilization approach reduces animal movement sufficiently to clearly image by eye and by camera.

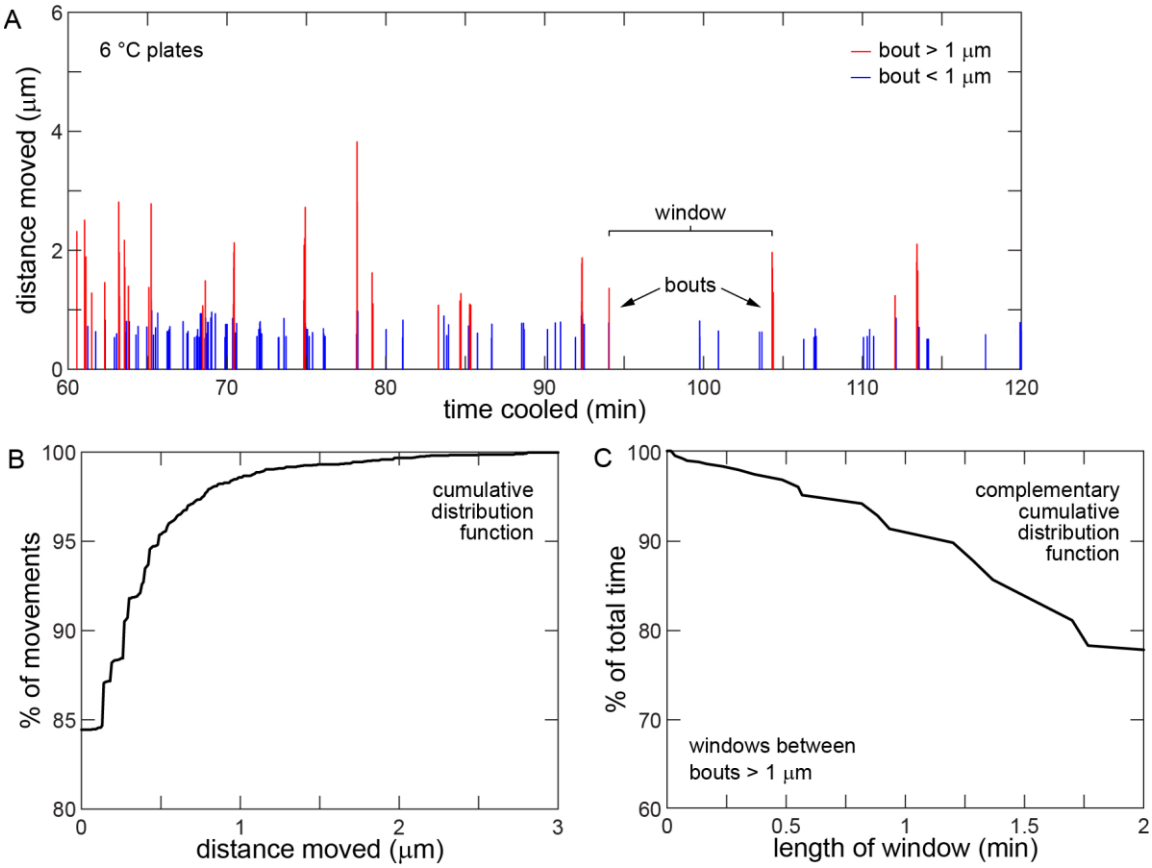

Fig. 5. Movement under cooling comprises intermittent bouts with long interstitial windows. (a) Movement measured each second reveals intermittent bouts of increased activity. Movements of < 1 μm do not produce significant image blur. (b) Cumulative distribution function of data in part A. Most movements are small: 99% of movements are < 1 μm. (c) Complementary cumulative distribution function of data in part A. Longer windows comprise most of experiment duration: 96% of duration is part of windows > 0.5 min long.

Touch stimulus temporarily reactivates movement

We next investigated the impact of touch stimulus on movement. Gentle and harsh touch to *C. elegans* alters the existing behavior of the animal and provokes an escape response (Chalfie, *et al.*, 2014; Chalfie and Sulston, 1981; Alkema, *et al.*, 2005). Likewise, touching animals in lethargus or sleep also reactivates them (Raizen, *et al.*, 2008; Iwanir, *et al.*, 2013). We immobilized animals using the slow cooling method to 6 °C and stimulated animals by moving them with a pick at 90 min (*i.e.*, harsh touch). As expected, touch stimulus reactivates immobilized animals (Fig. 6). Compared to the 10 min before touch

stimulus, velocity for the following 10 min is modestly elevated (p = 0.006) before returning to the immobilization baseline during the subsequent 10 min. Thus if animals are disturbed while immobilized, they may require a period of time before returning to full immobilization.

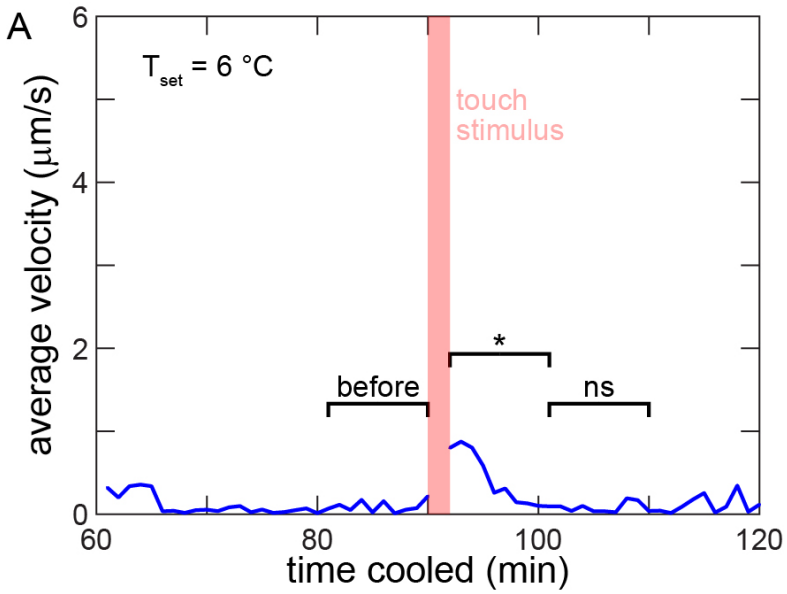

Fig. 6. Touch stimulus briefly reactivates movement. Nose tip velocity before and after harsh touch at 90 min are significantly different. Animals return to immobilization in 10 min. n = 6 animals. $p < 0.05$ (*).

Animals persist in immobilized state after temperature rises

We envision that, after a typical experiment involving cooling immobilization, plates can be moved back to their incubator to return animals to their cultivation temperature. We observed by eye the resumption of movement during warming on an inactive cooling stage. Because animals become strongly immobilized when cooled below 7 °C, we expected that movement would return at a similar temperature when warming animals to their cultivation temperature, 20°C. Intriguingly, following slow cooling immobilization and maintenance at 6 °C for 1 h, no animals resumed crawling before the plate temperature reached ~ 10 °C.

Even after the plate temperature reached 20 °C, at least 50% of animals remained immobilized until stimulated by gentle touch, whether externally applied or from contact with other animals moving on the plate. When stimulated by touch, animals transition within a few seconds directly from immobilized to crawling that appears normal by eye. Thus, while animals resume apparently normal behavior following cooling immobilization, the transition from immobilized to crawling may be more complex.

Cooling immobilization does not reduce lifespan or fecundity

Prior studies involving cooling of *C. elegans* indicate that cooling for shorter periods of time does not appear to impact the animal health (Rohde and Yanik, 2011), but longer periods (< 4 h) cause an immediate or progressive decline in health (Ohta, *et al.*, 2014; Robinson and Powell, 2016). We assayed viability and fecundity of animals immobilized by cooling for 1 h. First, we immobilized animals at 6 °C (slow cooling) and quantified their lifespan and number of offspring (Fig. 7). Lifespan and fecundity for control and cooled animals are not significantly different (black, blue data). Second, we immobilized animals at 1 °C (fast cooling) to test a harsher immobilization condition. Again, lifespan and fecundity for control and cooled animals are not significantly different (light gray, purple data). We conclude that cooling immobilization does not significantly affect animal health.

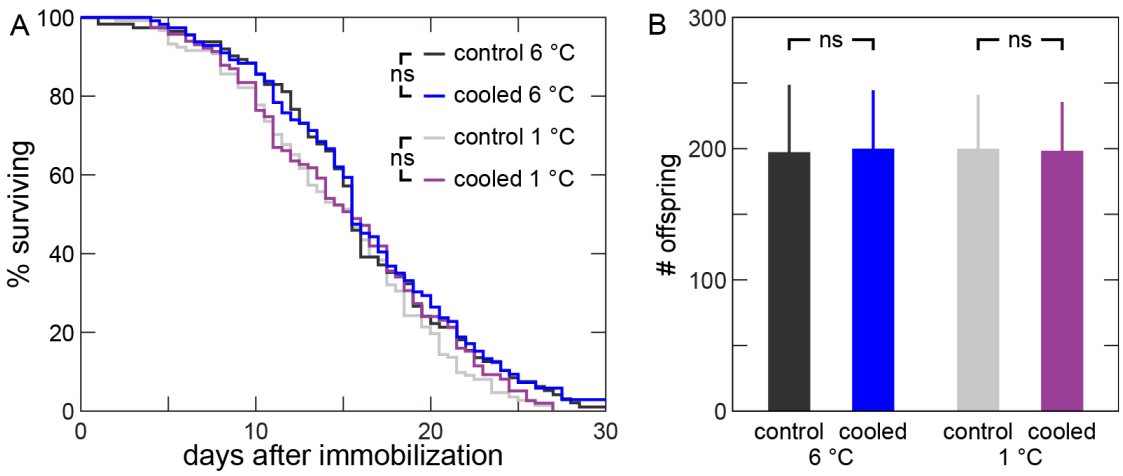

Fig. 7. Cooling immobilization does not reduce *C. elegans* lifespan and fecundity. Animal lifespan (a) and fecundity (b) after slow cooling to 6 °C or fast cooling to 1 °C, followed by 1 h at T_{set}. n = 110 (lifespan), 55 (fecundity) per condition. $p < 0.05$ (*) and $p < 0.001$ (**).

Timelapse imaging and 3D image stack

Illuminating animals with high intensity light stimulates movement in some animals. We describe our observations in the Discussion section. By eye, with our setup and animal strains, we note increased movement primarily when the illumination is focused to a size less than the animal length. Some animals remain motionless under illumination intensities sufficient for fluorescence imaging. By imaging animals immobilized on our cooling stage, we demonstrate high-resolution timelapse and z-stack images of individual neurons without movement-induced blurring. We obtained timelapse recordings (2 min length, 1 frame/s, 100-ms exposure) of an ASJ neuron expressing green fluorescent protein (GFP). By cross-correlation we tracked the movement of neuron structures within four areas in the field of view that focused on portions of the neuron (Fig. 8a). The distance the neuron structures moved from their position in the first frame is shown in Fig. 8b and is usually less than 0.2 μm. Thus, the distance moved during 2 min of imaging is below our resolution limit of 0.5 μm.

Incompletely immobilized animals produce images with blurred features due to motion during or between images. Blurring must be minimized or eliminated to obtain clear images, particularly for samples with fine features, such as the thin fibers of neurons. We took a z-stack of the ASJ neuron comprising 41 images with 1 μm step size taken at 1 slice every 4 s. As shown by the maximum projection of the z-stack in Fig. 8c, while there is haze around neuron structures from inherent out-of-focus and scattered light in widefield imaging (Wang, *et al.*, 2021), there is no image blur from motion. Specifically, the neuronal fibers are clearly resolved, even at high resolution. This clear image indicates minimal animal movement during 160 s of imaging, and it underscores the effectiveness of our instrument and approach for immobilization.

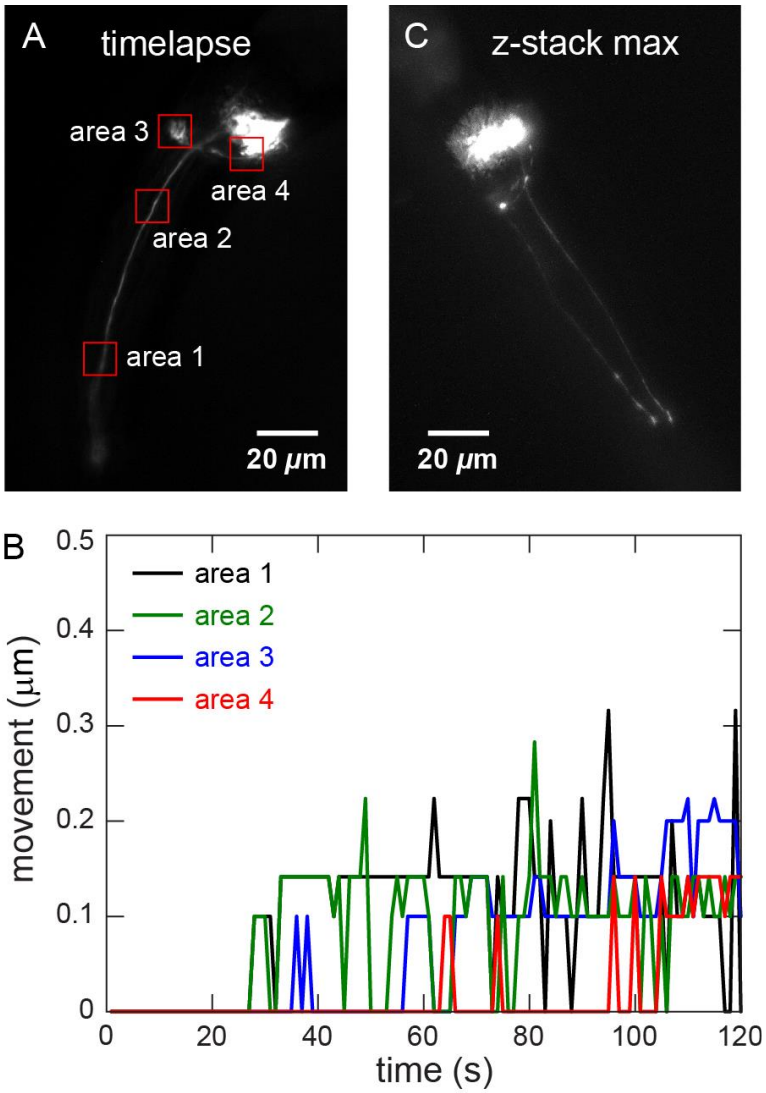

Fig. 8. High-resolution imaging under 6 °C cooling immobilization. Fluorescent *C. elegans* ASJ neuron imaged at 64× magnification. (a) Maximum projection of 2-min timelapse image sequence shows no motion blur. Relative movement of structures in areas 1-4 tracked by cross-correlation. (b) Minimal movement of structures in areas 1-4 during timelapse. (c) Maximum projection of 3D image stack acquired manually. Structures show no motion blur.

Discussion

Envisioned workflows

We envision two potential workflows utilizing our device to enable convenient, reversible immobilization of many animals for high-resolution imaging. In this study, we demonstrated the first workflow, where entire cultivation plates are cooled to 6 °C. Because

this method requires ~50 min to maximally immobilize animals, plates are "precooled" by placing them in a refrigerator for ~1 h, and subsequent cooling on the stage maintains the immobilization temperature. To maximize efficiency in multi-plate experiments, a plate is processed on the stage while simultaneously precooling the next plate that will be processed. Following imaging of immobilized animals, plates are returned directly to their incubator to bring them back to their cultivation temperature. The second workflow, involving a microchamber device for longitudinal imaging, is further described in the "Future Developments and Applications" section below.

Advantages of cooling stage and approach

Our cooling stage and approach have six technical capabilities, including some significant improvements over prior immobilization methods. First, large *C. elegans* populations are readily and reversibly immobilized by cooling. This immobilization allows observation, imaging, and manipulation of many animals over long time periods. Second, for some applications or genetic backgrounds, immobilization by cooling may be preferable to other methods due to secondary effects, such as stress response (Manjarrez and Mailler, 2020). For instance, chemical agents such as sodium azide induce stress proteins and thermotolerance in *C. elegans* (Massie, *et al.*, 2003). Third, our stage permits high-resolution fluorescence imaging of animals directly on cultivation plates. While *in vivo* microscopy on cultivation plates has been a mainstay technique for decades, it is more often performed by eye and at lower resolution. Our approach enables the study of subcellular processes and cell morphology without manipulating individual animals. Fourth, optical transparency of the sapphire window allows easy observation and imaging by brightfield transillumination, which is a primary method used for many imaging

applications in *C. elegans*. Fifth, we designed our cooling stage for straightforward installation into common upright microscope setups. The compact stage is very thin and is easily introduced into and removed from existing setups. Our cooling approach is also amenable to typical *C. elegans* experimental workflows. Finally, most immobilization techniques for high-resolution imaging do not easily allow animal reorientation while imaging. Our cooling stage maintains access to animals, which can be manipulated by a standard platinum pick throughout imaging, at the cost of time to reestablish full immobilization (see "Touch stimulus" section above). These six technical capabilities enable broad application of our device and approach to many problems that require high-resolution *in vivo* microscopy on large numbers of animals.

Our cooling stage and approach also has three practical, user-friendly features. First, our approach requires minimal user effort. Most other reversible immobilization techniques require transfer and manipulation of individual animals to complex setups or slides, which must also be fabricated. Our approach obviates this work by immobilizing animals on their cultivation plate. For high-resolution imaging experiments that involve animal recovery, we estimate that half the experimental time and a third of the user effort is expended in non-imaging activities such as animal handling, immobilization, and recovery (Chung, *et al.*, 2013b). Our full sodium azide immobilization procedure (Bargmann and Avery, 1995) requires ~160 min to process four batches of 25 animals each, not including time spent actually imaging animals. Our cooling immobilization procedure requires ~2 min, representing a savings of 98% of the active user time. Thus, our approach greatly accelerates the pace of experiments, enabling the straightforward application of high-resolution imaging to challenging procedures, such as screens. Second, our cooling stage

and approach are very simple and straightforward, and they require minimal training to operate. Some immobilization techniques involving complex setups require significant training and fine-tuning. In contrast our cooling stage has only a single voltage adjustment to control the immobilization temperature, and there are only two moving parts. Thus, our approach's simplicity makes it intuitive as well as resistant to failure. Finally, our device is accessible and inexpensive: we assembled it from easily attainable and affordable components, totaling a cost of ~$500. In summary, our device and approach have significant technical capabilities in a very user-friendly design.

Key technical developments and novel findings

In our study, we develop a novel, compact thermoelectric stage that cools entire cultivation plates to immobilize populations of *C. elegans* for imaging. Our stage cools plates to a uniform temperature distribution across the agar surface that is stable over long time periods. We describe animal movement under many cooling conditions in far greater detail than previously reported. We demonstrate that cooling has minimal impact on lifespan and fecundity. Our cooling stage successfully immobilizes animals sufficiently to allow high-resolution brightfield imaging. Despite some movement arising from high-intensity illumination for high-resolution fluorescence imaging, we demonstrate the capacity of our immobilization approach to perform time-lapse and z-stack fluorescence imaging. These techniques can be challenging as animal movement during the extended acquisition time blurs the images. In summary, our cooling stage represents a novel and effective way to reversibly immobilize large populations of *C. elegans* for high-resolution brightfield and fluorescence imaging.

During our study, we also encountered some interesting and unusual animal behavior. First, previous studies immobilized animals between 2-4 °C (Rohde and Yanik, 2011; Chung, *et al.*, 2008). By careful and systematic assay, we find that optimal immobilization of *C. elegans* occurs at a counterintuitively higher temperature of 5-7 °C after animals have been cooled for ~50 min. In contrast, animals cooled to 1-3 °C maintain a relatively stable level of movement that is significantly higher than at 6 °C. Animals held at 1 °C only slightly reduce their movement even after 2 h. In fact, a higher immobilization temperature is preferable as it is easier to maintain, has lower risk of freezing animals, and is presumably a more benign environment. Second, after cooling immobilization, many animals persist in the immobilized state even after warmed to cultivation temperatures but resume normal movement rapidly following gentle touch. Because animals immobilized by cooling also exhibit bouts of movement and respond to strong stimuli by temporary increased movement, we speculate that our immobilized state may be similar to sleep. Further studies are required to determine if cooling immobilization exhibits other hallmarks of sleep, or if it is more akin to partial anesthesia.

Limitations of cooling stage and approach

There are several limitations of our approach. First, animals raised at 15 °C continue to crawl at our standard immobilization temperature of 6 °C, indicating that cultivation temperature modulates cooling immobilization. This is not unexpected as prior studies have shown that raising *C. elegans* at colder temperatures improves cold tolerance (Murray, *et al.*, 2007). However, it does require additional fine-tuning of our approach if animals are not cultivated at 20 °C. Likewise we also speculate that some temperature-sensitive mutant strains of *C. elegans* may require adjustment of immobilization

temperature, as we have optimized our approach for the wild-type background. Second, the speed of immobilization is slower than most other methods, but we expect that the easy step of pre-cooling plates overcomes this weakness for most applications. Third, imaging fine structures at specific locations exhibiting greater movement, such as the dendritic cilia at the nose tip, could be challenging.

Finally, high-intensity illumination for fluorescence imaging at high-resolution stimulates movement in some animals. Our current investigations are aimed at quantifying and minimizing this effect. By eye, the nose appears to be more sensitive than the tail or the body to light. The location of GFP expression may affect light sensitivity as FLP-fluorescent animals could be illuminated with >10× more light than ASJ-fluorescent animals before stimulating movement. Also, green light illumination (red fluorescence imaging) triggers much less movement than blue light (green fluorescence imaging). These gradations of sensitivity are consistent with prior findings that neurons in the nose, and particularly the ASJ, contribute strongly to wavelength-dependent light sensitivity in *C. elegans* (Ward, *et al.*, 2008). Despite this sensitivity, we are still able to demonstrate high-resolution fluorescence imaging at the submicron level without motion blur.

Future developments and applications

Our cooling stage and associated equipment could be developed in several ways to greatly enhance its capabilities. A microfluidic or microchamber (Bringmann, 2011) device utilized with our cooling approach could permit longitudinal imaging of individual animals. A thin device would enable rapid, repeated cooling for brief imaging windows with minimal impact on animal health (Rohde and Yanik, 2011). Such a device would be

useful for tracking development or neuroregeneration following injury. Our study has also focused on imaging L4 and young adult animals; however, imaging and laser surgery on larval stages has been instrumental for understanding animal development and the roles of individual neurons. Larval stages are significantly more challenging to process for microscopy than later life stages, particularly the recovery step. If the procedure for cooling immobilization were optimized for larval stages, that would greatly facilitate larval imaging and laser surgery. In our study, we also completed procedures manually, but one advantage of our approach is that it is amenable to automation. Commercial plate handlers exist to move plates to instruments and could be easily adapted to load plates onto our cooling stage. The cooling immobilization and imaging could also be automated through multiple coolers and translation stages. There is also great potential for integrating our approach with image processing and segmentation algorithms to enable automated recognition of cellular components and targeting for laser surgery. The developments listed above would significantly extend the capabilities and accelerate the throughput of our platform allowing its application to a wide array of questions that are currently unapproachable.

Materials and Methods

Device design and components: We utilized Solidworks to design and model the thermal distribution of the cooling stage. Components: Peltier heat pump (CP854705-2, 40 × 40 mm, from CUI Devices, Lake Oswego in Oregon); 99.9% pure copper stage block (100 × 140 × 3 mm, machined); sapphire window (80 mm diameter, 3 mm thickness, from Altos Photonics, Bozeman in Montana); Thermal paste to connect parts (Arctic MX-4, from

Florence in South Carolina); liquid CPU Cooler (Hydro Series H100x, from Corsair, Fremont in California); copper liquid cooling heatsink (40 × 40 × 10 mm, replacing the original bulky heatsink, unbranded); custom installation bracket fabricated by FDM (Fused Deposition Modeling) 3D printing of polylactide filament.

Plate temperature measurements: We measured the thermal distribution of the agar plate using a calibrated thermal camera (Teledyne FLIR C2, Thousand Oaks in California). We embedded a wire digital thermocouple (Proster, San Jose in California) 1 mm into the agarose on plates to confirm camera readings and track agarose temperature over time.

Nematode handling: We maintained *C. elegans* on Bacto agar plates under standard conditions at 20 °C (Brenner, 1974). We utilized two strains in our study: a wild-type N2 strain and a fluorescent strain with *daf-11(sa195)V; ofIs1[ptrx-1::trx-1::gfp]* background. We utilized N2 for all experiments except for fluorescence imaging, where we utilized the fluorescent strain. We synchronized large populations of animals for experiments by placing ~30 adults on plates to lay eggs for 4 h. We transferred animals between plates using a pick. For the touch stimulus experiment, we used a pick to move animals at least 1 cm away from and then back to their original location.

Cooling methods: slow, fast, and abrupt

In general, the parameters of the cooling methods, such as voltages and times, that lead to the desired performance, will depend on specific parameters of the cultivation plates and stage, such as the amount of agar used to make the plates, the efficiency of the Peltier stage, and the material conductivities.

Slow cooling: In our study, we performed slow cooling to a target temperature (T_{set}) of 6 °C only. We first moved a 20 °C plate with to a 4 °C refrigerator for 1 h, with the plate's lid on. Then, we moved the plate directly to a cold stage (pre-cooled for 10 min with 4.8 V across the Peltier), with the plate's lid off for improved imaging and worm manipulation.

Fast cooling: We first moved a 20 °C plate with animals to a cold stage (cooled for 10 min at 12 V), with plate lid off. When the plate temperature reached T_{set} + 5 °C, we turned the voltage to a lower value (4.8 V for T_{set} = 6 °C and 7.1 V for T_{set} = 1 °C) to maintain plates at T_{set}. This method cools down plates to different target temperatures in ~15 mins.

Abrupt cooling: In our study, we performed abrupt cooling to 6 °C only. We moved animals from 20 °C plates to a pre-cooled 6 °C plate resting on the cooling stage.

Tip-Tracking: We first captured videos of animals under the stated conditions at 20 frames per second (FPS). Then, we extracted 1 frame per second from those videos using a custom MATLAB script. We manually tracked the nose tip position in those frames using the Multi-point Tool in ImageJ and calculated velocities for each second in MATLAB. We averaged the individual velocities of 60 s to produce average velocities for each minute.

Lifespan and fecundity analysis: We collected N2 wild-type animals in the L4 lifestage on two plates. We left the control plate in the cultivation incubator. The cooled plate was processed by the slow cooling to 6 °C and fast cooling to 1 °C methods described above. We held animals at T_{set} for 1 h. We then moved the cooled plate back to the cultivation incubator.

Lifespan: A few hours after treatment, we transferred animals to separate plates to avoid crowding. We observed animals twice daily following established procedure (Larsen, *et*

al., 1995) to assess mortality. We transferred animals to new plates when needed to avoid starvation.

Fecundity: A few hours after treatment, we transferred animals individually (*i.e.*, "singled") to plates. Three days later, we moved the singled animals to new plates and counted the number of hatched offspring for each animal. We repeated this process until there were no new offspring.

Timelapse and z-stack imaging: We used a Leica M205 FA fluorescence stereomicroscope with 5x, 0.5 numerical aperture (NA) objective to obtain z-stack and timelapse images. With other optics in the microscope body, we imaged green fluorescent protein at 64x magnification, with theoretical 0.5 μm transverse and 4 μm axial resolution. We performed both timelapse and z-stack fluorescence imaging on the *C. elegans* ASJ neuron. For timelapse imaging, we used 1 FPS with 100-ms exposure time for 2 minutes to obtain 120 frames in total. For z-stack imaging, we used a 3-axis stage (Thorlabs MBT616D, Newton in New Jersey) to obtain slices over a 40-μm z range, with 1-μm z step, 100-ms exposure time, and 4-s time interval between slices.

Statistics and interpretation of results: For comparing nose tip velocities, we calculated *p*-values using the *t* test: For different temperature settings or different cooling rates, we utilized the paired, two-tailed *t* test. For examining touch stimulus, we utilized the unequal variance, two-tailed *t* test.

For assessing the impact of cooling on viability and fecundity, we calculated *p*-value by using log-rank test and the unpaired, equal variance, two tailed *t* test, respectively. Data are

represented as average ± standard deviation (SD). In figures, we indicate values that differ significantly at $p < 0.05$ (*) and $p < 0.001$ (**) levels.

References

Alkema, M.J., Hunter-Ensor, M., Ringstad, N., and Horvitz, H.R. Tyramine Functions Independently of Octopamine in the Caenorhabditis elegans Nervous System. Neuron 46, 247-260 (2005). DOI: 10.1016/j.neuron.2005.02.024.

Bargmann, C.I., and Avery, L. Laser killing of cells in Caenorhabditis elegans. Methods Cell Biol 48, 225-250 (1995).

Basak, R., and Bandyopadhyay, R. Encapsulation of hydrophobic drugs in Pluronic F127 micelles: effects of drug hydrophobicity, solution temperature, and pH. Langmuir 29, 4350-4356 (2013).

Ben-Yakar, A., Chronis, N., and Lu, H. Microfluidics for the analysis of behavior, nerve regeneration, and neural cell biology in C. elegans. Curr Opin Neurobiol 19, 561-567 (2009). DOI: https://doi.org/10.1016/j.conb.2009.10.010.

Bowler, M.W., Montgomery, M.G., Leslie, A.G., and Walker, J.E. How azide inhibits ATP hydrolysis by the F-ATPases. Proceedings of the National Academy of Sciences 103, 8646-8649 (2006).

Brenner, S. The genetics of Caenorhabditis elegans. Genetics 77, 71-94 (1974).

Bringmann, H. Agarose hydrogel microcompartments for imaging sleep- and wake-like behavior and nervous system development in Caenorhabditis elegans larvae. J Neurosci Methods 201, 78-88 (2011). DOI: https://doi.org/10.1016/j.jneumeth.2011.07.013.

Chalfie, M., Hart, A.C., Rankin, C.H., and Goodman, M.B. Assaying mechanosensation. WormBook : the online review of C elegans biology, 10.1895/wormbook.1891.1172.1891 (2014). DOI: 10.1895/wormbook.1.172.1.

Chalfie, M., and Sulston, J. Developmental genetics of the mechanosensory neurons of Caenorhabditis elegans. Dev Biol 82, 358-370 (1981).

Chronis, N. Worm chips: microtools for C. elegans biology. Lab on a Chip 10, 432-437 (2010).

Chronis, N., Zimmer, M., and Bargmann, C.I. Microfluidics for in vivo imaging of neuronal and behavioral activity in Caenorhabditis elegans. Nat Methods 4, 727-731 (2007). DOI: 10.1038/nmeth1075.

Chuang, H.-S., Chen, H.-Y., Chen, C.-S., and Chiu, W.-T. Immobilization of the nematode caenorhabditis elegans with addressable light-induced heat knockdown (ALINK). Lab on a Chip 13, 2980-2989 (2013).

Chung, K.H., Crane, M.M., and Lu, H. Automated on-chip rapid microscopy, phenotyping and sorting of C. elegans. Nat Methods 5, 637-643 (2008). DOI: 10.1038/nmeth.1227.

Chung, S.H., Schmalz, A., Ruiz, R.C.H., Gabel, C.V., and Mazur, E. Femtosecond Laser Ablation Reveals Antagonistic Sensory and Neuroendocrine Signaling that Underlie C-elegans Behavior and Development. Cell Reports 4, 316-326 (2013a). DOI: 10.1016/j.celrep.2013.06.027. PMCID: PMC4780052.

Chung, S.H., Sun, L., and Gabel, C.V. In vivo Neuronal Calcium Imaging in C. elegans. Journal of Visualized Experiments, e50357 (2013b). DOI: 10.3791/50357. PMCID: PMC3653678.

Crane, M.M., Chung, K., Stirman, J., and Lu, H. Microfluidics-enabled phenotyping, imaging, and screening of multicellular organisms. Lab on a Chip 10, 1509-1517 (2010).

Dong, L., Cornaglia, M., Krishnamani, G., Zhang, J., Mouchiroud, L., Lehnert, T., Auwerx, J., and Gijs, M.A. Reversible and long-term immobilization in a hydrogel-microbead matrix for high-resolution imaging of Caenorhabditis elegans and other small organisms. PLOS ONE 13, e0193989 (2018).

Guo, S.X., Bourgeois, F., Chokshi, T., Durr, N.J., Hilliard, M.A., Chronis, N., and Ben-Yakar, A. Femtosecond laser nanoaxotomy lab-on-a-chip for in vivo nerve regeneration studies. Nat Methods 5, 531-533 (2008).

Hulme, S.E., Shevkoplyas, S.S., Apfeld, J., Fontana, W., and Whitesides, G.M. A microfabricated array of clamps for immobilizing and imaging C-elegans. Lab on a Chip 7, 1515-1523 (2007).

Iwanir, S., Tramm, N., Nagy, S., Wright, C., Ish, D., and Biron, D. The Microarchitecture of C. elegans Behavior during Lethargus: Homeostatic Bout Dynamics, a Typical Body Posture, and Regulation by a Central Neuron. Sleep 36, 385-395 (2013). DOI: 10.5665/sleep.2456.

Kim, E., Sun, L., Gabel, C.V., and Fang-Yen, C. Long-Term Imaging of Caenorhabditis elegans Using Nanoparticle-Mediated Immobilization. PLOS ONE 8, e53419 (2013). DOI: 10.1371/journal.pone.0053419.

Krajniak, J., Hao, Y., Mak, H.Y., and Lu, H. CLIP–continuous live imaging platform for direct observation of C. elegans physiological processes. Lab on a Chip 13, 2963-2971 (2013).

Krajniak, J., and Lu, H. Long-term high-resolution imaging and culture of C. elegans in chip-gel hybrid microfluidic device for developmental studies. Lab on a Chip 10, 1862-1868 (2010).

Larsen, P.L., Albert, P.S., and Riddle, D.L. Genes that regulate both development and longevity in Caenorhabditis elegans. Genetics 139, 1567-1583 (1995). DOI: 10.1093/genetics/139.4.1567.

Lockery, S. Channeling the worm: microfluidic devices for nematode neurobiology. Nat Methods 4, 691-692 (2007).

Manjarrez, J.R., and Mailler, R. Stress and timing associated with Caenorhabditis elegans immobilization methods. Heliyon 6, e04263 (2020). DOI: https://doi.org/10.1016/j.heliyon.2020.e04263.

Martin, R.J., Robertson, A.P., Buxton, S.K., Beech, R.N., Charvet, C.L., and Neveu, C. Levamisole receptors: a second awakening. Trends Parasitol 28, 289-296 (2012).

Massie, M.R., Lapoczka, E.M., Boggs, K.D., Stine, K.E., and White, G.E. Exposure to the metabolic inhibitor sodium azide induces stress protein expression and thermotolerance in the nematode Caenorhabditis elegans. Cell Stress Chaperones 8, 1-7 (2003).

Murray, P., Hayward, S.A.L., Govan, G.G., Gracey, A.Y., and Cossins, A.R. An explicit test of the phospholipid saturation hypothesis of acquired cold tolerance in Caenorhabditis elegans. Proceedings of the National Academy of Sciences 104, 5489-5494 (2007). DOI: 10.1073/pnas.0609590104.

Ohta, A., Ujisawa, T., Sonoda, S., and Kuhara, A. Light and pheromone-sensing neurons regulates cold habituation through insulin signalling in Caenorhabditis elegans. Nat Commun 5 (2014). DOI: 10.1038/ncomms5412.

Puttachary, S., Robertson, A.P., Clark, C.L., and Martin, R.J. Levamisole and ryanodine receptors (II): An electrophysiological study in Ascaris suum. Molecular and biochemical parasitology 171, 8-16 (2010).

Raizen, D.M., Zimmerman, J.E., Maycock, M.H., Ta, U.D., You, Y.J., Sundaram, M.V., and Pack, A.I. Lethargus is a Caenorhabditis elegans sleep-like state. Nature 451, 569-572 (2008). DOI: 10.1038/nature06535.

Reeve, E.C.R. The Nematode Caenorhabditis elegans . Edited by William B. Wood and the Community of C. elegans Researchers. New York: Cold Spring Harbor Laboratory, 1988. 667 pages. US $97.00. ISBN 0 87969 307 X. Genetics Research 52, 243-244 (1988).

Robertson, A.P., Clark, C.L., and Martin, R.J. Levamisole and ryanodine receptors (I): A contraction study in Ascaris suum. Molecular and biochemical parasitology 171, 1-7 (2010).

Robinson, J.D., and Powell, J.R. Long-term recovery from acute cold shock in Caenorhabditis elegans. BMC Cell Biol 17, 11 (2016). DOI: 10.1186/s12860-015-0079-z.

Rohde, C.B., and Yanik, M.F. Subcellular in vivo time-lapse imaging and optical manipulation of Caenorhabditis elegans in standard multiwell plates. Nat Commun 2, 7 (2011). DOI: 10.1038/ncomms1266.

Shachaf, Y., Gonen-Wadmany, M., and Seliktar, D. The biocompatibility of Pluronic® F127 fibrinogen-based hydrogels. Biomaterials 31, 2836-2847 (2010).

Wang, Y.L., Grooms, N.W.F., Civale, S.C., and Chung, S.H. Confocal imaging capacity on a widefield microscope using a spatial light modulator. PLOS ONE 16, e0244034 (2021). DOI: 10.1371/journal.pone.0244034. PMCID: PMC7886194.

Ward, A., Liu, J., Feng, Z.Y., and Xu, X.Z.S. Light-sensitive neurons and channels mediate phototaxis in C-elegans. Nat Neurosci 11, 916-922 (2008).

Zeng, F., Rohde, C.B., and Yanik, M.F. Sub-cellular precision on-chip small-animal immobilization, multi-photon imaging and femtosecond-laser manipulation. Lab Chip 8, 653-656 (2008).

.

Acknowledgments

Several people contributed to the work described in this paper. SHC conceived the idea. YLW, ELJ, and NWFG carried out experiments, and all authors analyzed the data. SHC supervised the experiments and the development of the manuscript. ELJ wrote the first draft of the manuscript; all authors subsequently took part in the revision process and approve the final copy of the manuscript.

We thank the members of the Chung Laboratory for feedback on the manuscript. We thank Neil Patel (Bioengineering, Northeastern Univ.) for assistance with animal nose tip tracking. We acknowledge Wenchao Zhu (Mechanical Engineering, Northeastern Univ.) for technical support in thermal distribution measurement. We acknowledge Xin Sun (Bioengineering, Northeastern Univ.) for technical support in 3D printing.

Movie S1. 20-min timelapse recording of immobilized animals. We acquired a 20-min long video of three wild type N2 animals immobilized on their cultivation plate under 6 °C, using 10 × magnification. We speed up the 20-min long video by 50× for audience watching convenience. Animal movements occur at times (s): Left animal nose tip- 99, 182, 392, 822, 1045; tail-359, 723. Center animal tail- 133, 297. Right animal nose tip- 0, 292, 469, 488.